Behavioral evidence for nested central pattern generator control of *Drosophila* grooming

Primoz Ravbar, Neil Zhang, Julie H. Simpson

Department of Molecular Cellular and Developmental Biology and Neuroscience Research Institute, University of California Santa Barbara
Corresponding authors: primoz.ravbar@gmail.com and jhsimpson@ucsb.edu

Abstract

Central pattern generators (CPGs) are neurons or neural circuits that produce periodic output without requiring patterned input. More complex behaviors can be assembled from simpler subroutines, and nested CPGs have been proposed to coordinate their repetitive elements, simplifying control over different time-scales. Here, we use behavioral experiments to establish that *Drosophila* grooming may be controlled by nested CPGs. On the short time-scale (5-7 Hz), flies execute periodic leg sweeps and rubs. More surprisingly, transitions between bouts of head cleaning and leg rubbing are also periodic on a longer time-scale (0.3 - 0.6 Hz). We examine grooming at a range of temperatures to show that the frequencies of both oscillations increase – a hallmark of CPG control – and also that the two time-scales increase at the same rate, indicating that the nested CPGs may be linked. This relationship also holds when sensory drive is held constant using optogenetic activation, but the rhythms decouple in spontaneously grooming flies, showing that alternative control modes are possible. Nested CPGs simplify generation of complex but repetitive behaviors, and identifying them in *Drosophila* grooming presents an opportunity to map the neural circuits that constitute them.

Introduction

Animals combine simpler movements into complex routines, forming behaviors with organization across multiple time-scales. For example, a California spiny lobster explores its olfactory environment by waving different segments of its antenna with different frequencies: slow and broad oscillations originating from the base allow the antenna to cover a large space around the animal. The next segment oscillates a little faster, ensuring optimal sampling for local exploration, and the most distal segments, where the sensory organs are located, oscillate fastest, adding fine granularity to the lobster's olfactory image of the world (Ravbar, field observations). How is this complex behavior assembled from simpler movements in such a harmonious manner?

Central pattern generators (CPGs) are neural circuits that produce rhythmic motor outputs in response to a trigger without requiring ongoing descending drive or patterned sensory inputs (Hooper & Büschges, 2017). CPGs control short stereotypic actions in cat walking, crayfish swimming, locust flight, leech heartbeat, and the stomatogastric and pyloric rhythms of crustaceans (reviewed in (Berkowitz, 2019; Grillner, 2006; Marder & Calabrese, 1996; Mulloney & Smarandache, 2010; Selverston, 2010)). However, CPGs may also contribute to control more complex behaviors. When the movements that compose a behavior repeat, it is inefficient to execute each step with a separate decision. Automating

the sequence by calling its actions in series produces reliable control. Increasingly complex sequences can be assembled from shorter elements, suggesting hierarchical control. When repetitive subroutines are themselves composed of simpler periodic movements, it has been suggested that they may be controlled by nested CPGs, hierarchically organized so that a "high-level" slow CPG controls the behavior on coarse scale and a "lower-level" fast CPG adds the fine structure (Berkowitz, 2019). In other words, the slow CPG controls alternations *between* subroutines and the fast CPG controls alternations *within* these subroutines. Various combinations of coarse and fine oscillators could produce behaviors of arbitrary complexity while still keeping them well-timed, stereotyped, and coherent. Bird song, for example, contains sound syllables executed in sequences. The syllables are short repeating elements, and sequences of syllables make phrases or words that also repeat, creating structure over several time-scales. Ingenious local cooling experiments of specific brain regions cause the whole song to slow down, indicating that it is governed by central pattern generating circuits (Long & Fee, 2008).

Here we show that *Drosophila* grooming behavior contains patterned elements over several time-scales: a fast repeat of individual leg movements (sweeps or rubs) and a slow alternation between bouts of head cleaning and front leg rubbing. We demonstrate that both of these repeated elements show evidence of CPG control, and that the two rhythms are usually coordinated, establishing fly grooming as a model system for understanding the circuit architecture of nested CPGs.

Results

Two time-scales of grooming are periodic

When flies are covered in dust, they initially groom anterior body parts using their front legs (Seeds et al., 2014). They alternate between series of head sweeps, where the legs move synchronously, and bouts of leg rubbing, where the legs move in opposition to each other, scraping the dust off. These movements are shown schematically in **Figure 1A**: the purple and orange arrows indicate parallel and anti-parallel leg movements and the thicker blue arrow shows the alternation between those leg coordination modes. Bouts of head cleaning (h) are indicated in purple and front leg rubbing (f) in orange on the ethogram (record of behavior actions over time) shown in **Figure 1B**.

The individual leg sweeps and rubs are stereotyped: the repeated bouts of these movements are recognizable by human observers or machine vision algorithms (Ravbar, Branson, & Simpson, 2019), and they represent the short time-scale we consider here. We can count individual leg movements from raw videos (see Methods) and thus compute their frequencies. In **Figure 1C** we show an example of frequencies of leg sweeps and rubs during the same period as **Figure 1A-B**. We demonstrate their periodicity using autocorrelation analysis (**Figure 1F** and **G)**. At 18ºC, as shown here, leg rubs and sweeps have a characteristic frequency ~6Hz. This means that each complete leg movement takes approximately 150 msec to complete, which is consistent with our unpublished observations using higher resolution camera recordings. The periodicity of the short time-scale leg sweep and rub movements suggests that they are produced by central pattern generating circuits, a hypothesis we will test further below.

Grooming is not a fixed action pattern and flies choose subroutines such as anterior grooming or wing cleaning stochastically, but with different levels of prioritization (Seeds et al., 2014). They typically make several head sweeps in a row, followed by repeated leg rubbing movements; we call these chunks

of repeated actions *bouts*. We use our Automatic Behavior Recognition System (ABRS; (Ravbar et al., 2019)) to automatically classify different grooming actions and to identify the time-points of maximum confidence as the centers of bouts (orange and purple circles in **Figure 1D**). Head cleaning bouts and front leg rubbing bouts alternate, and we define the time between two head cleaning bouts as an *hh-cycle* while the time between two consecutive front leg rubbing bouts is an *ff-cycle*. These terms are illustrated in **Figure 1E**, and cycles are the long time-scale we investigate here.

Although previous work revealed some syntactic organization at the bout level – both identity and duration of current action influence the identity and duration of the next (Mueller, Ravbar, Simpson, & Carlson, 2019) - we were surprised to find that the alternation of head cleaning and front leg rubbing bouts is periodic. Autocorrelation analysis of the ff-cycles shown in **Figure 1H** demonstrates signal at ~0.45 Hz, corresponding to approximately 2 seconds between the mid-point of consecutive bouts of front leg rubbing. Similar periodicity is observed for hh-cycles (data not shown.)

The discovery that both short time-scale and long time-scale subroutines within grooming behavior show periodicity suggests the possibility that they may both be controlled by central pattern generating circuits. The proposal that nested CPGs simplify the control of repetitive motor sequences (Berkowitz, 2019) is an appealing framework to explain rhythmicity in complex behaviors such as grooming that occur on multiple time-scales. We now consider the response of these rhythms to increasing temperature as additional evidence that central pattern generators govern both time-scales, and to determine whether the two levels of the proposed nested CPGs are independent or interlocked.

The period lengths of both time-scales contract with increasing temperature

A key feature of central pattern generators is that they oscillate faster at higher temperatures (Deliagina, Orlovsky, & Pavlova, 1983; Tang et al., 2010). To determine whether temperature affects periodicity of leg sweeps and rubs (short time-scale) or the alternation between bouts of head sweeps and leg rubs (ff-cycles; long time-scale), we recorded the grooming behavior of dust-covered flies at a range of temperatures between 18 and 30ºC. Example ethograms from the extreme temperatures are shown in **Figure 2A**, and the entire dataset arranged from coolest to warmest temperature is displayed in **Figure 2B**. This represents 84 individual flies at seven temperatures recorded for 13 minutes each.

Temperature increase causes faster individual leg movements (**Figure 2C-E**) in both sweeps and rubs (**Supplementary Figure 1**). The oscillation remains periodic (**Supplementary Figure 2**), and the frequency of leg movements across temperatures shows a linear increase from 5.8Hz to 6.8Hz (R^2=0.99, $p<0.001$) (**Figure 2D-E**). When we examine how the autocorrelations change with time (**Supplementary Figure 3**) we observe rich structure, on at least the short time-scale (x-axis) and the long time-scale (y-axis), that contracts with temperature in both dimensions.

Crucially, the period of long time-scale movements is also compressed by temperature. The ff-cycle frequency increases from 0.45Hz at 18ºC to 0.53Hz at 30ºC, also in a linear manner ($p<0.001$, R^2=0.98; **Figure 2F-H**). The frequencies of hh-cycles show a very similar trend (**Supplementary Figure 4**). This result suggests that CPGs may be involved in the generation of the long time-scale alternations. The autocorrelations for the long time-scale are more variable, and the behavior is more ragged at higher temperature (**Supplementary Figure 2D**). This is consistent with previous evidence in other models

that central pattern generators are less stable at elevated temperature (Alonso & Marder, 2020; Rinberg, Taylor, & Marder, 2013).

Increasing temperature shortens the cycle period of both the short time-scale leg sweeps and rubs and the long time-scale alternation between bouts of head cleaning and front leg rubbing, corroborating the hypothesis that both time-scales are controlled by two levels of nested CPGs. Now we ask whether these two time-scales contract together (at the same rate), which would suggest a mechanistic linkage between the two levels.

Two time-scales contract together, suggesting connections between nested CPGs

Several metrics indicate that the short and long time-scales contract at the same rate as temperature increases, suggesting that their control mechanisms are linked. We noticed that the number of leg movements within a ff-cycle is fairly consistent (average ~12). **Figure 3A** demonstrates that this average number of leg movements holds, even as the speed ff-cycles increases with temperature: at 18ºC, there are 12 leg movements of 170 msec for a ff-cycle duration of 2.17 seconds, while at 30ºC there are 12 leg movements of 148 msec for a ff-cycle duration of 1.89 seconds. Thus, the average number of leg movements per ff-cycle remains the same across all temperatures (**Figure 3B**), supporting the hypothesis that the two levels of nested CPGs controlling the short and long time-scales are linked.

An alternative way to determine whether the two time-scales scale together with temperature is to plot their contraction *rates*. By normalizing by their minimal frequencies, we can visualize the slope of temperature dependence for each time-scale: the correlation is striking ($p<0.002$, $R^2=0.94$; **Figure 3C)**. Both time-scales contract at the same rate, with R^2 values of 0.96 and 0.93, respectively. Similar trends can be seen for hh-cycles (**Supplementary Figure 5**). Together these data support the hypothesis that the short time-scale leg movements and the long time-scale alternations between anterior grooming subroutines are controlled by two levels of nested central pattern generating circuits.

Periodicity and correlation between time-scales persist when sensory stimulation is constant

So far, we have shown that two hallmarks of CPGs – periodicity and temperature-dependent frequency increase – hold for both short time-scale leg sweeps or rubs and long time-scale alternations between leg rubbing and head cleaning subroutines. An additional criterion for determining if a behavior is controlled by a CPG is that rhythmic output does not require rhythmic or patterned input. When flies are covered in dust, their grooming actions alter the sensory input. The faster their legs sweep, the more quickly dust is removed. Perhaps the coupling between time-scales can be explained because faster leg sweeps result in more dust removal, which reduces sensory drive and thus shortens grooming bouts. In other words, the rhythmic behavioral output could result in similarly rhythmic sensory input - thus not excluding the reflex chain explanation of the observed periodicity (Marder & Bucher, 2001). What happens to the periodicity of long time-scale, across temperatures, if the sensory drive is held constant? We predict that if the long time-scale is indeed CPG-controlled, it should contract with increasing temperature even when we hold the sensory input constant. We test this using optogenetic activation of all mechanosensory bristle neurons.

We previously demonstrated that this manipulation induces grooming, beginning with the anterior body parts, and alternating between bouts of head cleaning and front leg rubbing (Hampel, McKellar, Simpson, & Seeds, 2017; Zhang, Guo, & Simpson, 2020). Here, we combine optogenetic activation for

constant sensory input with temperature control to show that both individual leg movements and bout-level alternations increase in a correlated manner. Representative ethograms at 18º and 30ºC show characteristic alternation between bouts of head cleaning and front leg rubbing (**Figure 4A**). The entire dataset of optogenetically-induced grooming over a range of temperatures is shown in **Figure 4B**. Uniform sensory input evokes rhythmic output at both short and long time-scales (long time-scale shown in **Supplementary Figure 6**) and the period of these rhythms gets shorter with temperature (**Figure 4C-H)**. The frequency of ff-cycles increases significantly ($R^2 = 0.82$, p=0.02) with temperature and leg movement frequencies increase somewhat less ($R^2 = 0.70$, p=0.08, respectively). The frequencies are similar to dust-induced grooming and the average number of leg movements per ff-cycle is also similarly preserved across the range of temperatures (**Figure 4I-J**). As with dusted flies, the rate of contraction of the two time-scale is correlated (**Figure 4K**), supporting the hypothesis that the short time-scale leg movements and the long time-scale bout alternations are both controlled by CPGs, and that these circuits are yoked together.

Optogenetic stimulation of mechanosensory neurons does not precisely mimic the physical stimulus of dust itself, and the response of the optogenetically manipulated flies to temperature reflects this. Both short and long time-scale behaviors occur with somewhat shorter periodicity at lower temperature than their dust-evoked counterparts and stop increasing beyond 26-28º C (compare **Figures 2E, H** and **4E, H**). One possible explanation is that the optogenetic stimulation is "maxing out" the sensory input: it may be driving the fastest leg movements biomechanically possible, or the upper bound of the CPG's frequency range may be reached at a lower temperature. Starting from the higher frequency baseline, the two time-scales still increase with temperature at similar rates (**Figure 4K**).

Nested CPGs can be decoupled in spontaneously grooming flies

Flies groom robustly in response to dust or optogenetically-controlled mechanosensory stimulation, but they also groom spontaneously. The leg movements they perform are recognizable sweeps and rubs, and they occasionally produce alternating bouts of head cleaning and front leg rubbing as well (**Figure 5A, B**). These flies have no sensory stimuli except what they generate themselves by contact between their legs and bodies, so any motor patterns may be coordinated by internal circuits. We analyzed the temperature response of both time-scales of grooming movements in spontaneously grooming flies.

Although these flies groom less than dusted or optogenetically-activated flies, they show characteristic sweep and rub frequencies that increase with temperature, with higher variance (5.5Hz to 7.2Hz; **Figure 5B, D-F**). The ff-cycles are rarer, and when they occur, the temperature-dependent contraction is much less pronounced (**Figure 5C, G,** and **H**). Although the number of leg movements per ff-cycle is similar to stimulated flies (~14; with higher variation across the temperature range, **Figure 5I, J**), the correlated temperature-dependent contraction of the short and long time-scale observed in the dusted and optogenetically activated flies is not seen in the spontaneously grooming ones (compare **Figure 5K** to **Figures 3K** and **4K**). Leg rubs and sweeps increase with temperature at a greater rate than ff and hh-cycles (**Figure 5K**), suggesting that the pattern-generating circuits that control the two time-scales of movements can be dissociated in spontaneous grooming. Perhaps some aspects of grooming, namely the bouts of head cleaning or front leg rubbing, can be either driven rhythmically by a high-level CPG (as they seem to be in stimulated flies) or initiated individually in a less patterned way, in spontaneously grooming flies.

Discussion

Temperature manipulations have been instrumental in identifying behaviors controlled by central pattern generators and for locating where those circuits reside. Robust rhythms are retained across a range of temperatures in the stomatogastric ganglia, where the relative timing of events is preserved even as the sequence itself changes speeds (Alonso & Marder, 2020; Rinberg et al., 2013; Tang, Taylor, Rinberg, & Marder, 2012). Local cooling of the cat spinal cord demonstrated which segments contain locomotion control circuits (Deliagina, Orlovsky, & Pavlova, 1983), and local warming showed that cricket chirping is governed by thoracic rather than brain ganglia (Pires & Hoy, 1992a, 1992b). The role of CPGs in bird song, and the importance of the HVC brain region for sequence duration, was shown because local cooling expands the entire song without changing the relative timing of the syllable components (Armstrong & Abarbanel, 2016; Long & Fee, 2008). Here, we examine fly grooming behavior at different temperatures to demonstrate that both its short and long time-scale components show evidences of CPG control.

Fly grooming is an innate motor sequence with both repetition and flexibility. Behavior analysis has shown organization over several time-scales, from single stereotyped leg movements, to alternation between bouts of repeated actions targeting a specific body part (Mueller, Ravbar, Simpson, & Carlson, 2019), to a gradual and probabilistic progression from anterior toward posterior grooming (Seeds et al., 2014). Here we investigate what aspects of fly grooming are periodic, demonstrating that the short time-scale leg sweeps and rubs repeat at characteristic frequencies, in the absence of patterned sensory input, and in a temperature-dependent manner (**Figures 2-5**), consistent with control by a central pattern generator. Since the neural circuits that constitute the CPGs that control these periodic leg movements are likely to overlap with those proposed to coordinate walking (Bidaye, Bockemuhl, & Buschges, 2018), this was expected.

But our more surprising discovery was that the alternation between bouts of head cleaning and front leg rubbing is also periodic. While this oscillation is more variable, it too, is: (1) independent of patterned sensory input, and (2) it increases in frequency with temperature (**Figures 2-5)** – strongly suggesting that there may be an additional CPG circuit operating at this longer time-scale. Thus, this high-level, overarching, CPG can control the alternations between leg rubs and sweeps that are themselves governed by a faster, low-level CPG. The concept of multiple CPGs to coordinate movements is not new. CPGs may control each leg joint, regulating the interaction between flexor and extensor muscles, controlling the way coxa-trochanter and femur-tiba joints are coordinated to produce forward or backward walking, or mediating interactions among limbs (Feng et al., 2020; Mantziaris, Bockemuhl, & Buschges, 2020). In the vertebrate spinal cord, inhibitory and excitatory commissural neurons can cause the CPGs controlling the legs to synchronize for a hopping gait or operate out-of-phase for walking (Kiehn, 2016). This concept of nested CPGs has recently been extended to explain flexible coordination of behaviors ranging from fish swimming to bird song (Berkowitz, 2019). In a recent publication, a very similar nested CPG to the one we are proposing here has been described in the crab stomatogastric ganglion where fast pyloric and slow gastric mill rhythms are coupled (Powell, Haddad, Gorur-Shandilya, & Marder, 2020). We map fly grooming behavior into this framework in **Figure 6.**

The combination of two rhythmic behaviors raises the possibility that the governing circuits interact, like meshed gears of different sizes, to simplify control of a repetitive behavior or to compensate for

temperature changes. Just as the relative number of rotations between different gears is the same regardless of the absolute speed of the mechanism, so is the phase of different components of CPGs conserved across a range of temperatures (Marder & Bucher, 2001). And in the case of fly grooming this relationship between fast and slow components of the system may be reflected in the conserved number of leg movements in a grooming bout across a range of temperatures (**Figure 3, Figure 4 I-K, Supplementary Figure 5**). But the neural circuit implementation of nested CPGs, and the "clutch" mechanisms that engage and disengage their connections, has not yet been determined.

Dust-induced grooming can be routine, rhythmic, repetitive, governed by central pattern generators, but spontaneous grooming may have different control architecture. Fast walking insects may be more likely to engage CPGs, while slower ones may rely more on sensory feedback and reflex chains (Mantziaris, Bockemuhl, & Buschges, 2020). Just as you can walk a straight path without thinking about it or you can carefully place each foot on icy terrain, flies may have alternative ways to produce grooming. Disturbing a single bristle elicits a single directed leg sweep (Kays, Cvetkovska, & Chen, 2014; Vandervorst & Ghysen, 1980), while covering the fly in dust evokes an entire grooming program with bouts of several leg sweeps and rubs, the alternations between the bouts and gradual progression from mostly anterior to mostly posterior behaviors (Phillis et al., 1993; Seeds et al., 2014). So our observation that spontaneous grooming does not show strong periodicity of the long time-scale can be interpreted as effective decoupling of the two levels of the nested CPG in those flies that engage in more sporadic and shorter episodes of grooming behaviors.

The specific neural circuits that constitute CPGs have been challenging to identify in most preparations and even the best characterized would benefit from more comparators. The electrophysiological recordings that have been so critical in CPG analysis in other preparations are possible but challenging in *Drosophila*, but the real strength of the system is the ability to demonstrate that specific neurons have a causal connection to rhythm generation. New anatomical resources to map neural circuits, especially the complete electron microscopy dataset covering the ventral nerve cord (Maniates-Selvin et al., 2020), will enable identification of the pre-motor neurons most likely to participate in CPGs and the commissural connections that may mediate among them. Functional imaging on neural activity in dissected, fictively moving preparations (Pulver et al., 2015) and even in behaving flies (Chen et al., 2018) is another promising approach to identify neurons with rhythmic activity that many constitute parts of the central pattern generators. The genetically encoded calcium indicators and new voltage indicators have fast enough onset and offset kinetics to capture rhythmicity on the expected time-scales (Simpson & Looger, 2018). Rhythmic activity and circuit connectivity may suggest candidate neurons; the genetic tools to target specific neurons (Jenett et al., 2012) and the optogenetic methods to impose altered activity patterns (Klapoetke et al., 2014) presents a way to causally connect specific neurons to control of rhythmic behaviors.

The behavioral evidence presented here suggests that nested CPGs can control aspects of fly grooming. The leg rubbing and bout alternations usually scale together in respond to temperature but can decouple in spontaneous grooming. Identifying what circuits constitute these central pattern generators and mapping the neurons that coordinate their interactions to produce fly grooming is feasible, now that we know we ought to be looking for them.

Acknowledgements

We thank members of the Simpson, Louis, and Kim labs for feedback, and especially Li Guo and Dr. Josh Mueller for excellent suggestions.

Methods

Fly stocks and husbandry

Drosophila melanogaster were reared on common cornmeal food in a 25°C incubator on a 12 hr light/dark cycle. 3-5 days CantonS males were used for dusting and spontaneous grooming experiments. For optogenetic experiments, larvae were raised on normal food. After eclosion, 1-day old adults were transferred into food containing 0.4 mM all-trans-retinal and reared in the dark for another two days. R74C07-GAL4 (attp2) was obtained from Bloomington Stock Center (Bloomington, IN).

Behavior experiments with temperature control

Behavior videos were recorded inside New Brunswick I2400 incubator shaker or DigiTherm DT2-MP-47L heating/cooling incubator. Experiments were performed every 2°C between 18°C and 30°C. Temperature was monitored by a Govee H5072 Bluetooth thermometer. For dusting experiments, the room temperature was also adjusted to target temperature to make sure flies stay at the same temperature during fly dusting. Each fly was tested once in one condition. Three chambers were used in fly dusting assay: dusting chamber (24 well corning tissue culture plate #3524), transfer chamber and recording chamber. Flies were anesthetized on ice and transferred to the middle four wells of the transfer chamber. Transfer chamber with flies was then kept in the incubator set to the target temperature for 15 min. For fly dusting, around 5 mg Reactive Yellow 86 dust was added into each of the 4 middle wells of the dusting chamber. Transfer chamber was aligned with the dusting chamber. Flies were tapped into the dusting chamber and shaken for 10 times. After dusting, flies and dust were transferred back into the transfer chamber. Transfer chamber was banged against an empty pipette tip box to remove extra dust. Dusted flies were then immediately tapped into the recording chamber for video recording. The whole dusting process was performed in a Misonix WS-6 downflow hood.

For optogenetics and spontaneous grooming experiments, ice-anesthetized flies were put into the recording chamber directly. Recording chamber with flies was then kept in the incubator set to the target temperature for 15 min before experiment. In spontaneous grooming experiments, flies were shaken for 5 times after the 15 min incubation. They were then rested in the incubator for another 3 minutes before recording.

60 Hz videos were recorded for 9 min in optogenetics experiments, 13 min in dusting and spontaneous grooming experiments with a FLIR Blackfly S USB 3 camera. Infrared backlight was used for all experiments. Custom-made LED panels (LXM2-PD01-0050, 625nm) were used for optogenetic activation from below. 20 Hz 20% light duty cycle was used in optogenetics experiments. Red light intensity was adjusted to 0.85 mW/cm^2.

Leg movements counting from video

Regions of interest were cropped around the animals to produce 80x80 arrays of pixels (**F**). The **F** arrays were reshaped into 1600 rows and 30 rows, corresponding to 30 consecutive frames (1 sec window), were stacked together to obtain 30x1600 array of pixel values (**W**).

The derivatives of **W** across time were computed using Numpy.gradient() function to obtain matrix of frame-to-frame differences **D**. The matrix **D** was smoothed using Gaussian filter (`scipy.ndimage.filters.gaussian_filter`). This was done to denoise the signal - to remove non-biological high frequency changes.

All the values of **D** where cumulative change of pixel values was less than threshold ($\theta = 5.0$) were converted to zeros to retain only those pixels where significant movement occurred.

Peaks of significant changes, corresponding to animal movements were found using `scipy.signal.find_peaks()` function on the matrix **D**. The number of peaks is assumed to be the number of leg sweeps that occurred in the time window (.5 sec). This was justified because only the frames where grooming behavior was detected were considered for leg sweep counting. The number of leg movements per second was used as the leg movement frequency.

Automatic behavior recognition from videos

Probabilities and ethograms of grooming behaviors were extracted from raw videos using Automatic Behavior Recognition System (ABRS). For detailed description see (Ravbar et al., 2019) and for the most updated version see ABRS (https://github.com/AutomaticBehaviorRecognitionSystem/ABRS)

Briefly, ABRS pre-processes video data by compressing it into spatio-temporal features in the form of 3-channel space-time images (3CST images, shape=80 x 80 x 3) where the first channel [0] contains raw video frame pixel values [80x80], the second channel [1] contains spectral features of pixel value dynamics over a time-window of 16 frames, and the third channel [2] contains frame-to-frame difference (frame subtraction). The 3CST images are classified into 7 behavioral categories (front leg rubbing, head cleaning, back leg rubbing, abdominal cleaning, wing cleaning and whole-body movements (walking)) by ConvNet (Covolutional Neural Network - CNN) implemented in Tensor Flow, (in Python) (https://www.tensorflow.org) using a model trained with diverse set of videos of fly grooming behaviors. In the final output layer of the CNN are the probabilities of the grooming behaviors. In this work we focus entirely on the probabilities of front leg rubbing and head cleaning behaviors: P(f) and P(h).

Behavioral confidence

The long time-scale oscillations are quantified as probabilities of behaviors obtained from the ABRS CNN described above. Behavioral confidence is computed as:

$$BC = P(f) - P(h) \qquad \text{Eq. 1}$$

Autocorrelation analysis

Autocorrelation functions (ACFs) were computed from a 0.5 sec time-window for individual leg movements (leg rubs and sweeps). The signal for autocorrelation was extracted from raw movies as follows: 1) Matrix **D** was obtained as described above (Leg movements counting from video); 2) ACFs were computed for every column of **D**; and 3) All the ACFs were averaged to obtain the mean ACF for that time-window. The mean ACFs were stacked to obtain the ACF array with dimensions 60 x F, where F is the number of frames in the movie. The AFCs were computed using `scipy.signal.correlate` function from SciPy library.

Autocorrelation functions (ACFs) for the long time-scale (the oscillations between bouts of leg rubbing and head cleaning) were computed from the behavioral confidence (BC) time-traces described in Eq.1, in the time-window of 999 frames (16.6 sec), also using the `scipy.signal.correlate` function.

Frequency computations for the long time-scales

Behavioral confidence (BC) traces were used to compute the frequencies of the long time-scale.

$$f = 1/L \qquad \text{Eq.2}$$

In Eq. 2 the L is a vector containing the lengths of periods measured from the BC traces. The periods were measured either between two peaks of the BC traces (ff-cycles) or between two valleys (hh-cycles) (also see **Figure 1E** for illustration). This produced a vector of frequencies of dimensions 1xF, where F is the number of frames in a movie, corresponding to one fly. The mean and median frequencies for each fly were computed as means/medians of vector *f*.

Handling of outliers and missing data points

We found and did not eliminate an outlier in optogenetically stimulated flies (leg movement frequencies at 20ºC). In cases where there were missing data points (no fly was in the recording chamber), those were not counted in the statistics.

References

Alonso, L. M., & Marder, E. (2020). Temperature compensation in a small rhythmic circuit. *Elife, 9*. doi:10.7554/eLife.55470

Armstrong, E., & Abarbanel, H. D. (2016). Model of the songbird nucleus HVC as a network of central pattern generators. *J Neurophysiol, 116*(5), 2405-2419. doi:10.1152/jn.00438.2016

Berkowitz, A. (2019). Expanding our horizons: central pattern generation in the context of complex activity sequences. *J Exp Biol, 222*(Pt 20). doi:10.1242/jeb.192054

Bidaye, S. S., Bockemuhl, T., & Buschges, A. (2018). Six-legged walking in insects: how CPGs, peripheral feedback, and descending signals generate coordinated and adaptive motor rhythms. *J Neurophysiol, 119*(2), 459-475. doi:10.1152/jn.00658.2017

Chen, C. L., Hermans, L., Viswanathan, M. C., Fortun, D., Aymanns, F., Unser, M., . . . Ramdya, P. (2018). Imaging neural activity in the ventral nerve cord of behaving adult Drosophila. *Nat Commun, 9*(1), 4390. doi:10.1038/s41467-018-06857-z

Deliagina, T. G., Orlovsky, G. N., & Pavlova, G. A. (1983). The capacity for generation of rhythmic oscillations is distributed in the lumbosacral spinal cord of the cat. *Exp Brain Res, 53*(1), 81-90. doi:10.1007/BF00239400

Feng, K., Sen, R., Minegishi, R., Dübbert, M., Bockemühl, T., Büschges, A., & Dickson, B. J. (2020). Distributed control of motor circuits for backward walking in Drosophila. *bioRxiv*, 2020.2007.2011.198663. doi:10.1101/2020.07.11.198663

Grillner, S. (2006). Biological pattern generation: the cellular and computational logic of networks in motion. *Neuron, 52*(5), 751-766. doi:10.1016/j.neuron.2006.11.008

448 Hampel, S., McKellar, C. E., Simpson, J. H., & Seeds, A. M. (2017). Simultaneous activation of parallel
449 sensory pathways promotes a grooming sequence in Drosophila. *Elife, 6*.
450 doi:10.7554/eLife.28804
451 Jenett, A., Rubin, G. M., Ngo, T. T., Shepherd, D., Murphy, C., Dionne, H., . . . Zugates, C. T. (2012). A
452 GAL4-driver line resource for Drosophila neurobiology. *Cell Rep, 2*(4), 991-1001.
453 doi:10.1016/j.celrep.2012.09.011
454 Kays, I., Cvetkovska, V., & Chen, B. E. (2014). Structural and functional analysis of single neurons to
455 correlate synaptic connectivity with grooming behavior. *Nat Protoc, 9*(1), 1-10.
456 doi:10.1038/nprot.2013.157
457 Kiehn, O. (2016). Decoding the organization of spinal circuits that control locomotion. *Nat Rev*
458 *Neurosci, 17*(4), 224-238. doi:10.1038/nrn.2016.9
459 Klapoetke, N. C., Murata, Y., Kim, S. S., Pulver, S. R., Birdsey-Benson, A., Cho, Y. K., . . . Boyden, E.
460 S. (2014). Independent optical excitation of distinct neural populations. *Nat Methods, 11*(3), 338-
461 346. doi:10.1038/nmeth.2836
462 Long, M. A., & Fee, M. S. (2008). Using temperature to analyse temporal dynamics in the songbird
463 motor pathway. *Nature, 456*(7219), 189-194. doi:10.1038/nature07448
464 Maniates-Selvin, J. T., Hildebrand, D. G. C., Graham, B. J., Kuan, A. T., Thomas, L. A., Nguyen, T., . . .
465 Lee, W.-C. A. (2020). Reconstruction of motor control circuits in adult Drosophila using
466 automated transmission electron microscopy. *bioRxiv*, 2020.2001.2010.902478.
467 doi:10.1101/2020.01.10.902478
468 Mantziaris, C., Bockemuhl, T., & Buschges, A. (2020). Central pattern generating networks in insect
469 locomotion. *Dev Neurobiol, 80*(1-2), 16-30. doi:10.1002/dneu.22738
470 Marder, E., & Calabrese, R. L. (1996). Principles of rhythmic motor pattern generation. *Physiol Rev,*
471 *76*(3), 687-717. doi:10.1152/physrev.1996.76.3.687
472 Mueller, J. M., Ravbar, P., Simpson, J. H., & Carlson, J. M. (2019). Drosophila melanogaster grooming
473 possesses syntax with distinct rules at different temporal scales. *PLoS Comput Biol, 15*(6),
474 e1007105. doi:10.1371/journal.pcbi.1007105
475 Mulloney, B., & Smarandache, C. (2010). Fifty Years of CPGs: Two Neuroethological Papers that
476 Shaped the Course of Neuroscience. *Front Behav Neurosci, 4*. doi:10.3389/fnbeh.2010.00045
477 Phillis, R. W., Bramlage, A. T., Wotus, C., Whittaker, A., Gramates, L. S., Seppala, D., . . . Murphey, R.
478 K. (1993). Isolation of mutations affecting neural circuitry required for grooming behavior in
479 Drosophila melanogaster. *Genetics, 133*(3), 581-592. Retrieved from
480 https://www.ncbi.nlm.nih.gov/pubmed/8454205
481 Pires, A., & Hoy, R. R. (1992a). Temperature coupling in cricket acoustic communication. I. Field and
482 laboratory studies of temperature effects on calling song production and recognition in Gryllus
483 firmus. *J Comp Physiol A, 171*(1), 69-78. doi:10.1007/BF00195962
484 Pires, A., & Hoy, R. R. (1992b). Temperature coupling in cricket acoustic communication. II.
485 Localization of temperature effects on song production and recognition networks in Gryllus
486 firmus. *J Comp Physiol A, 171*(1), 79-92. doi:10.1007/BF00195963
487 Powell, D. J., Haddad, S. A., Gorur-Shandilya, S., & Marder, E. (2020). Coupling between fast and slow
488 oscillator circuits in *Cancer borealis* is temperature compensated. *bioRxiv*,
489 2020.2006.2026.173427. doi:10.1101/2020.06.26.173427
490 Pulver, S. R., Bayley, T. G., Taylor, A. L., Berni, J., Bate, M., & Hedwig, B. (2015). Imaging fictive
491 locomotor patterns in larval Drosophila. *J Neurophysiol, 114*(5), 2564-2577.
492 doi:10.1152/jn.00731.2015

Ravbar, P., Branson, K., & Simpson, J. H. (2019). An automatic behavior recognition system classifies animal behaviors using movements and their temporal context. *J Neurosci Methods, 326*, 108352. doi:10.1016/j.jneumeth.2019.108352

Rinberg, A., Taylor, A. L., & Marder, E. (2013). The effects of temperature on the stability of a neuronal oscillator. *PLoS Comput Biol, 9*(1), e1002857. doi:10.1371/journal.pcbi.1002857

Seeds, A. M., Ravbar, P., Chung, P., Hampel, S., Midgley, F. M., Jr., Mensh, B. D., & Simpson, J. H. (2014). A suppression hierarchy among competing motor programs drives sequential grooming in Drosophila. *Elife, 3*, e02951. doi:10.7554/eLife.02951

Selverston, A. I. (2010). Invertebrate central pattern generator circuits. *Philos Trans R Soc Lond B Biol Sci, 365*(1551), 2329-2345. doi:10.1098/rstb.2009.0270

Simpson, J. H., & Looger, L. L. (2018). Functional Imaging and Optogenetics in Drosophila. *Genetics, 208*(4), 1291-1309. doi:10.1534/genetics.117.300228

Tang, L. S., Taylor, A. L., Rinberg, A., & Marder, E. (2012). Robustness of a rhythmic circuit to short- and long-term temperature changes. *J Neurosci, 32*(29), 10075-10085. doi:10.1523/JNEUROSCI.1443-12.2012

Vandervorst, P., & Ghysen, A. (1980). Genetic control of sensory connections in Drosophila. *Nature, 286*(5768), 65-67. doi:10.1038/286065a0

Zhang, N., Guo, L., & Simpson, J. H. (2020). Spatial Comparisons of Mechanosensory Information Govern the Grooming Sequence in Drosophila. *Curr Biol, 30*(6), 988-1001 e1004. doi:10.1016/j.cub.2020.01.045

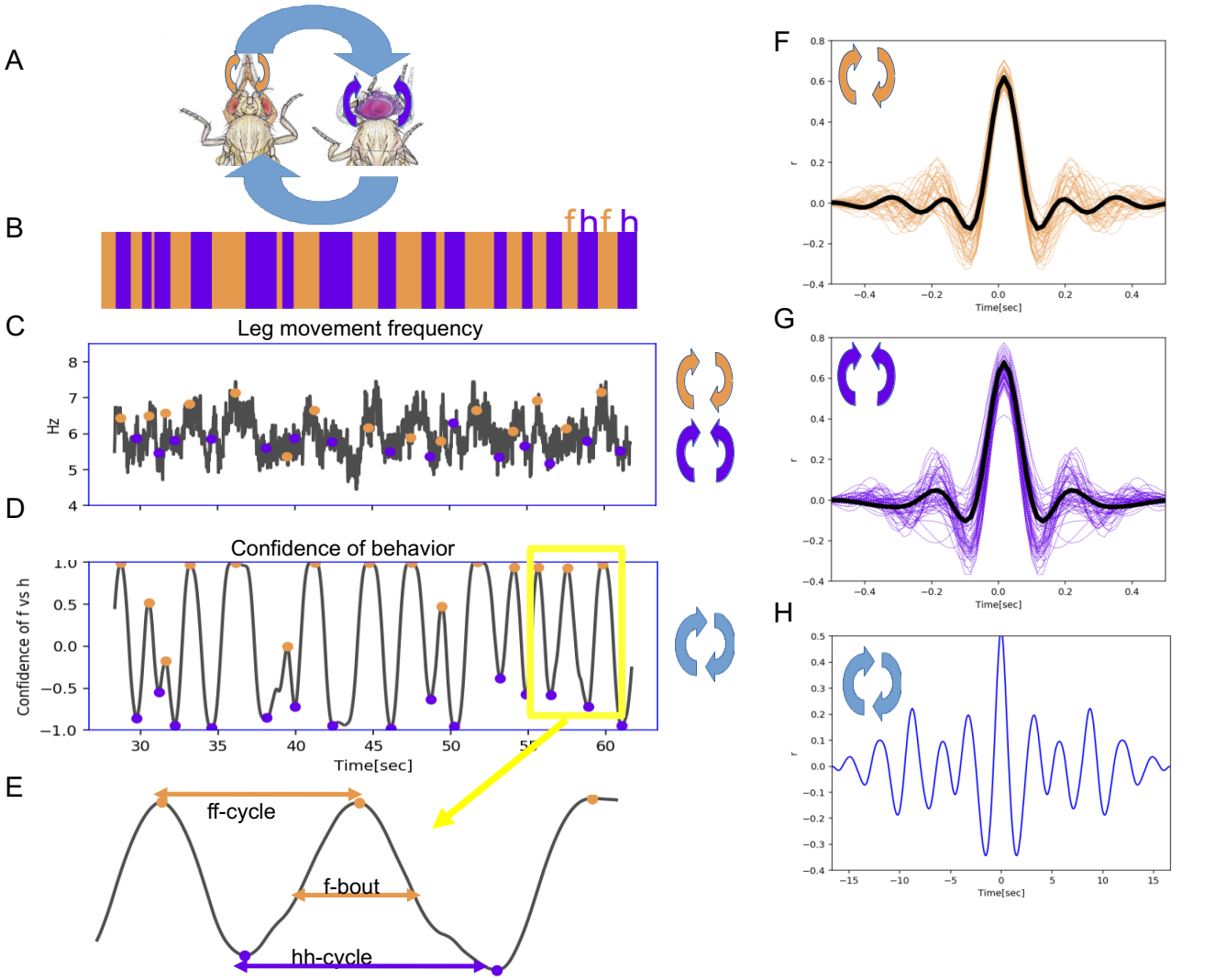

Figure 1: Two time-scales of grooming behavior are periodic.

(**A**) Schematic of anterior grooming behavior. The anti-parallel motion of leg rubbing is indicated by the orange arrows and parallel head cleaning movements are indicated by purple arrows (the short time-scale). The blue arrows indicate alternations between the leg rubbing and head cleaning subroutines (the long time-scale). (**B**) Ethogram showing alternations between bouts of front leg rubbing (f) and head cleaning (h) in dust-covered flies recorded at 18ºC. (**C**) Example leg sweep and rub frequencies measured in the 30 seconds of anterior grooming behavior shown in the ethogram above. Purple and orange dots indicate front leg rubbing (f) and head cleaning (h) as detected by the Automatic Behavior Recognition System. (**D**) Bouts of front leg rubbing (f) or head cleaning (h) are identified by their probabilities (from the output of the Convolutional Neural Network). When we subtract the probability of h-bouts from that of f-bouts, we obtain the confidence of behavior curve shown here (see Methods). Purple and orange dots indicate maxima and minima of confidence in behavior identification, corresponding to the centers of the f- and h- bouts respectively. (**E**) Enlarged segment taken from (**D**) showing the definitions of ff- and hh-cycles and f-/h- bouts. (**F**) Samples of autocorrelation functions (ACF) computed from over 3 minutes of movies when the fly was engaged in front leg rubbing or head sweeps (**G**). The thick black lines indicate the average of these samples, while thinner purple and orange lines represent each individual ACF contributing to this average.; see Methods for details. (**H**) Autocorrelation function of the alternation of f and h bouts from the example of ff-cycles shown in **D** also reveals periodic signal.

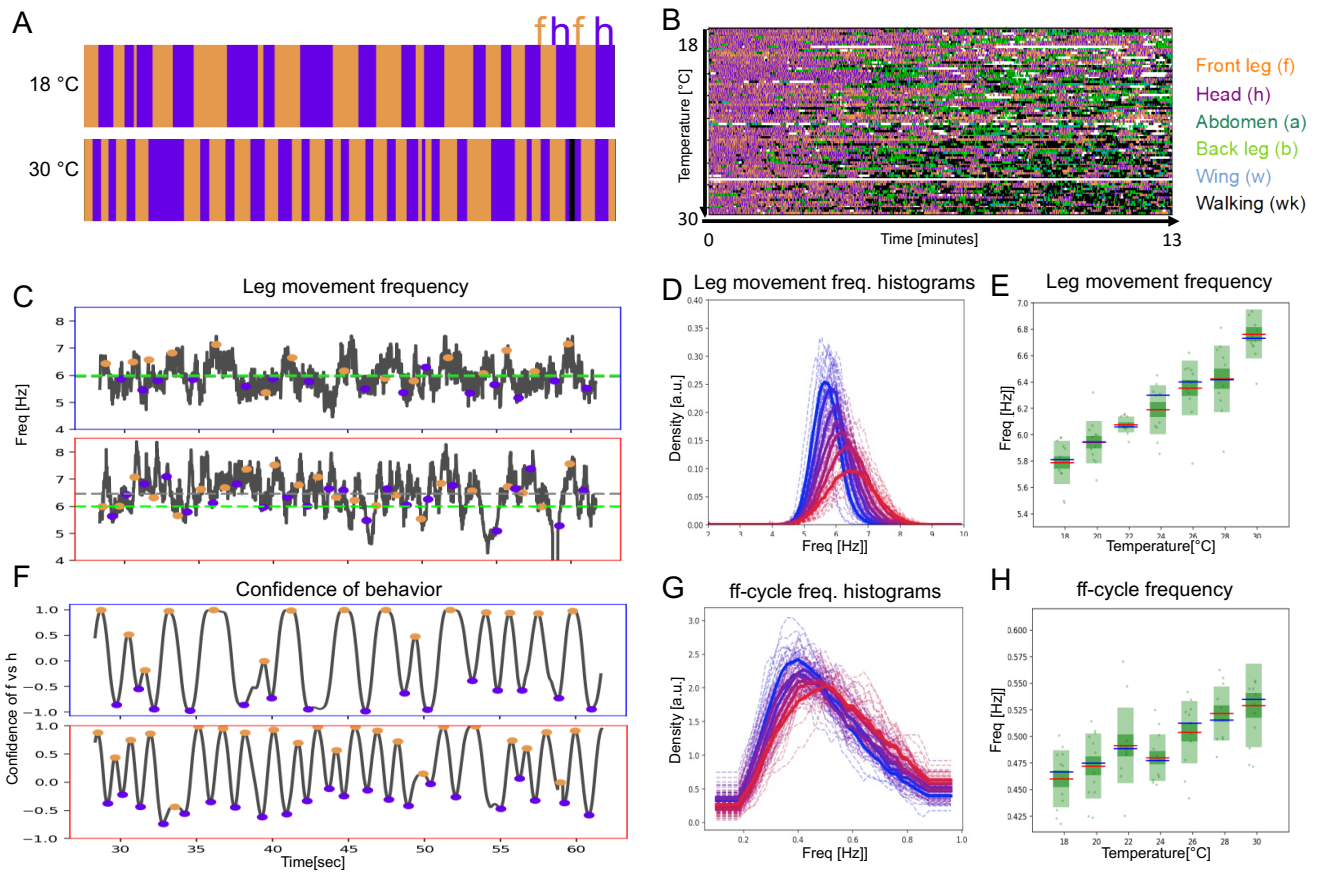

Figure 2: Period lengths of two time-scales contract with increasing temperature in dust-stimulated flies

(**A**) Examples of ethograms recorded at 18ºC (top) and 30ºC (bottom). (**B**) Ethograms of 84 dust-stimulated flies recorded at different temperature (18 – 30ºC). Colors represent behaviors as indicated in the color legend on the right. (**C**), **(D),** and (**E**) The frequency of individual leg movements increases with temperature. (**C**) Shows example frequency time series from 30 seconds of grooming at 18º (top, blue outline) and 30ºC (bottom, red outline). Gray dashed line = mean of this sample; green dashed line = reference at 6 Hz. (**D**) Histogram of leg movement frequencies, sampled from seven temperatures (18º - 30ºC.) Lower temperatures are indicated in blue and higher ones in red. Thin lines – individual histograms; thick lines – average of samples at each temperature. All histograms are computed from the 84 ethograms of dust-stimulated flies in (**B**). (**E**) Box plots of leg sweep frequencies. Dots show individual fly averages, while the blue bars show the mean frequency, the red bars mark median and the green shaded areas indicate standard deviation (SD) and error (Blue/red bars in box plots – mean/median; shaded areas – SD and SE). (**F**), (**G**) and (**H**) The frequency of ff-cycles also increases with temperature. (**F**) As described in **Figure 1D,** this plot shows the confidence, in samples recorded at 18ºC (top) and 30ºC (bottom). (**G**) and (**H**): Similar to the panels (**D**) and (**E**) but showing the increase of ff-cycle frequency with temperature computed from the 84 dust-stimulated flies.

See **Supplementary Figures 1, 2, 3** and **4**

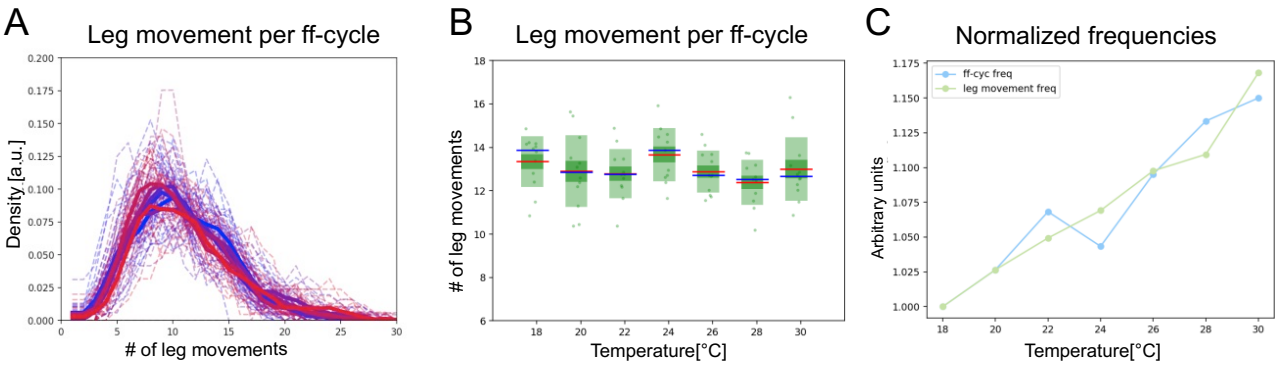

Figure 3: The two time-scales contract together with increasing temperature.

(**A**) Histograms of numbers of leg movements per ff-cycle in cooler temperatures (blue) and warmer temperatures (red). (**B**) Box plots of leg movement counts per ff-cycle across the seven temperatures; statistics as in **Figure 2E.** (**C**) The frequency of individual leg movements and bout alternations (ff-cycles) increases roughly linearly with temperature but over different time-scales (msec vs. sec; 7 Hz vs. 0.5 Hz). To see if they increase at the same rate, we compare them in arbitrary units. Frequencies were normalized by dividing each mean value from **Figure 2E** by the lowest value recorded: this produces the rate of change, where 1.0 means no change and values above 1.0 reflect the increased rate.

See **Supplementary Figure 5** for similar effects in hh-cycles.

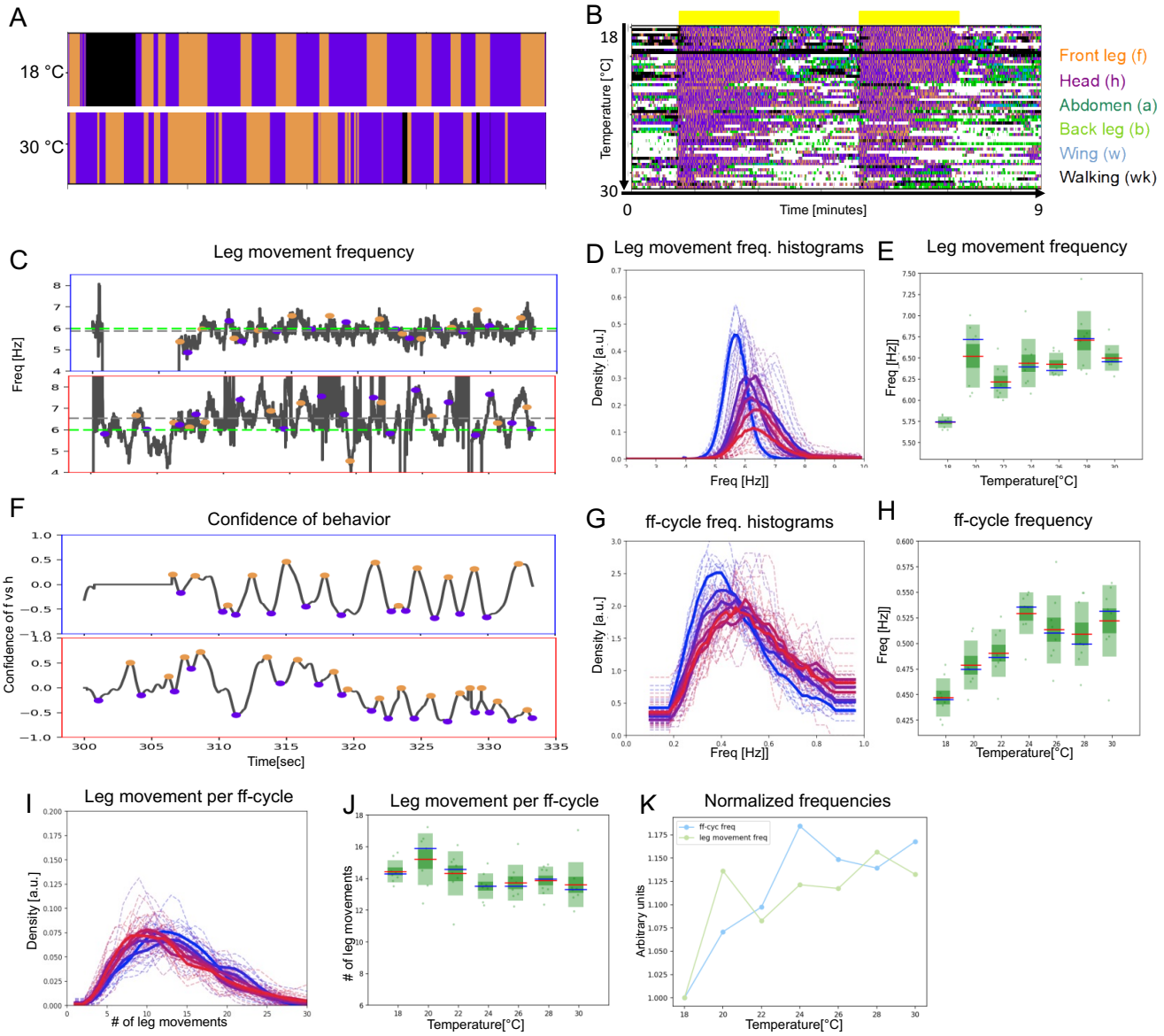

Figure 4: Under constant sensory stimulation, the temperature effect on both time-scales persists

Undusted flies expressing the optogenetic activator *UAS-Chrimson* in mechanosensory bristles were stimulated with red light to induce anterior grooming behavior. Examples ethograms recorded at 18º (top) and 30ºC (bottom) are shown in (**A**), while (**B**) shows the whole dataset of ethograms representing 56 flies across the range of temperatures, similar to **Figure 2D**. The yellow bars represent the periods of light activation, lasting 2 minutes each, to optogenetically induce grooming. (**C**) Examples of leg movement frequencies at 18º (top) and 30ºC (bottom), (**D**) histograms of mean frequencies at cool (blue) and warm (red) temperatures, and (**E**) box plots of the increase in leg movement frequency with temperature; plots and statistics as described in **Figure 2C, D,** and **E**; compare to short time-scale effects where grooming is induced by dust. (**F, G** and **H**) Long-time scale ff-cycle analysis same as in **Figure 2F, G** and **H**. **(I)** Histograms and box plots (**J**) of median leg movement counts per ff-cycle across the seven temperatures, quantified as in **Figure 3A** and **B.** (**K**) The rate of temperature-driven increase in frequency is shown by normalization as in **Figure 3C**.

See **Supplementary Figure 6** for similar results on hh-cycles.

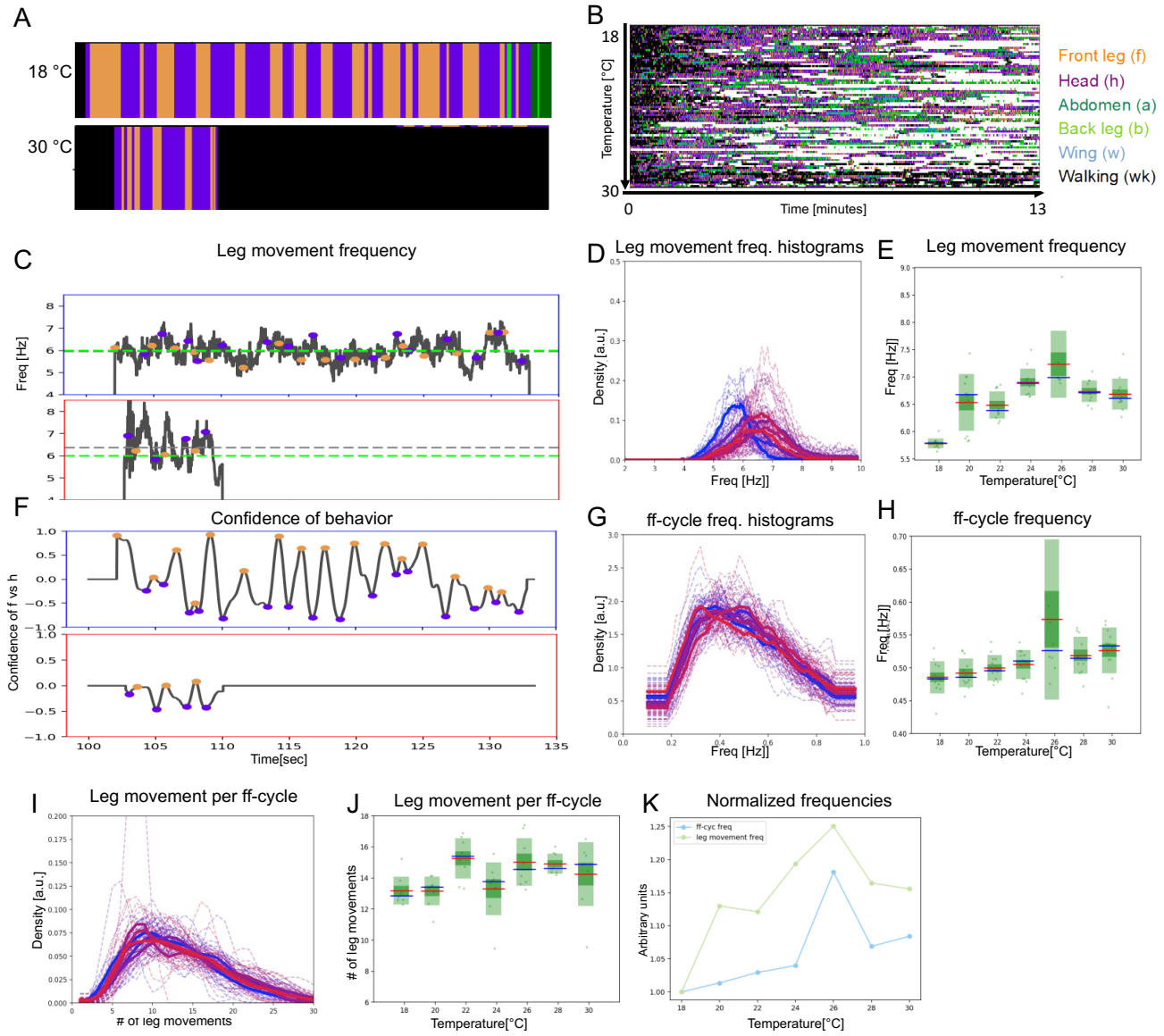

Figure 5: The two time-scales of patterned movements can be decoupled in spontaneous grooming

Spontaneous grooming was recorded in undusted flies at a range of temperatures between 18º and 30ºC. Examples are shown in (**A**) and the whole dataset of 80 flies recorded for 13 minutes is shown in (**B**). (**C**) Examples of spontaneous leg movement frequencies at 18º (top) and 30ºC (bottom), (**D**) histograms of mean frequencies at cool (blue) and warm (red) temperatures, and (**E**) box plots of the increase in leg movement frequency with temperature; plots and statistics as described in **Figure 2** and **3C, D,** and **E**; compare to short time-scale effects where grooming is induced by dust. (**F, G** and **H**) Long-time scale ff-cycle analysis comparable to **Figure 2** and **3F, G** and **H**. **(I)** Histograms and box plots (**J**) of median movement counts per ff-cycle across the seven temperatures, quantified as in **Figure 3A** and **B.** (**K**) The rate of temperature-driven increase in frequency is shown by normalization as in **Figure 3C**.

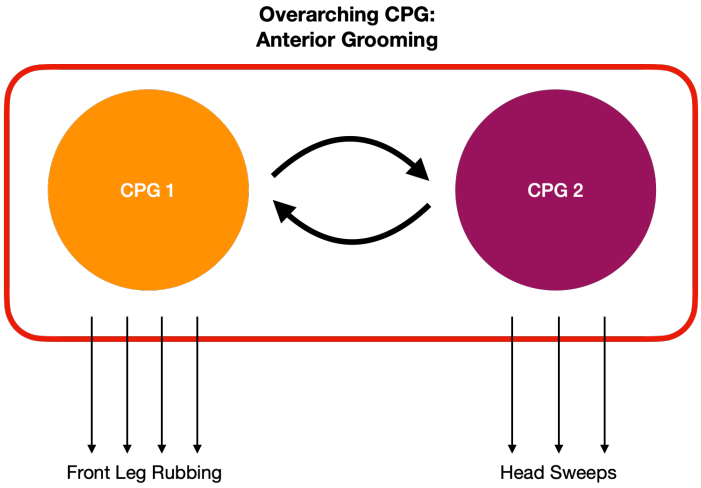

Figure 6: Schematic of nested CPG controlling anterior grooming behavior

Adapted from the concept of hierarchical CPGs shown in (Berkowitz 2019) Figure 4, this diagram illustrates how CPGs controlling individual leg rubbing and leg sweeping movements can be coordinated by an over-arching CPG controlling the alternation of front leg rubbing and head cleaning bouts. Leg rubbing occurs at slightly higher frequency than leg sweeps, indicated by the number of arrows produced by CPG 1 vs. 2 during each bout (indicated by colored circles).

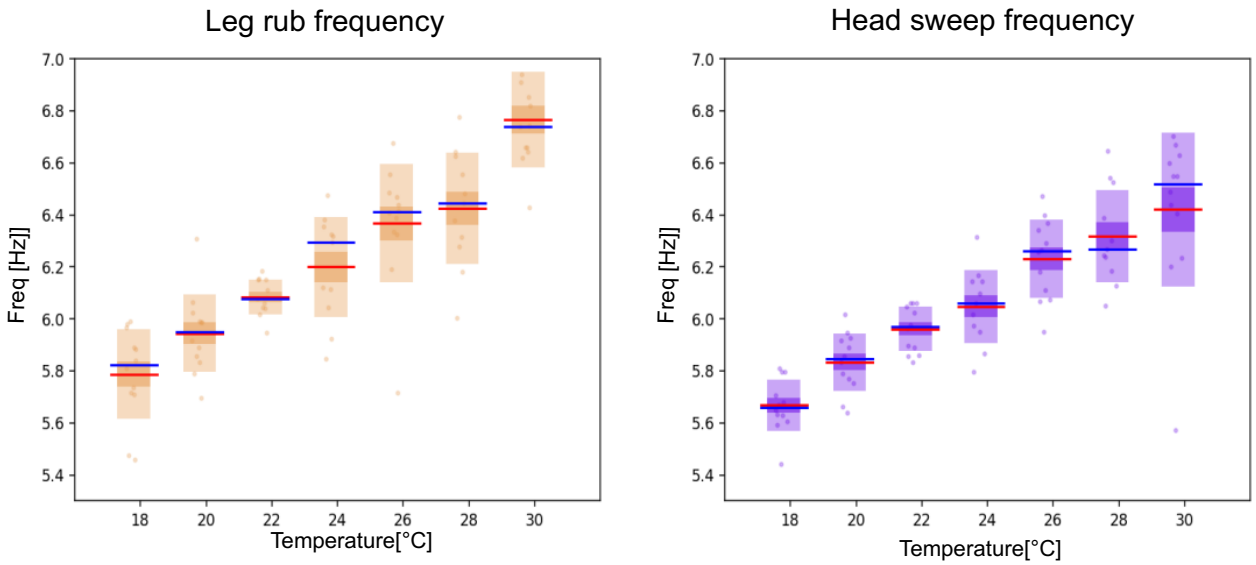

Supplementary Figure 1: Frequencies of leg rubs and head sweeps increase with temperature

Separating the individual leg movements into leg rubs and head sweeps shows that the frequency of both increases with temperature at a similar rate.

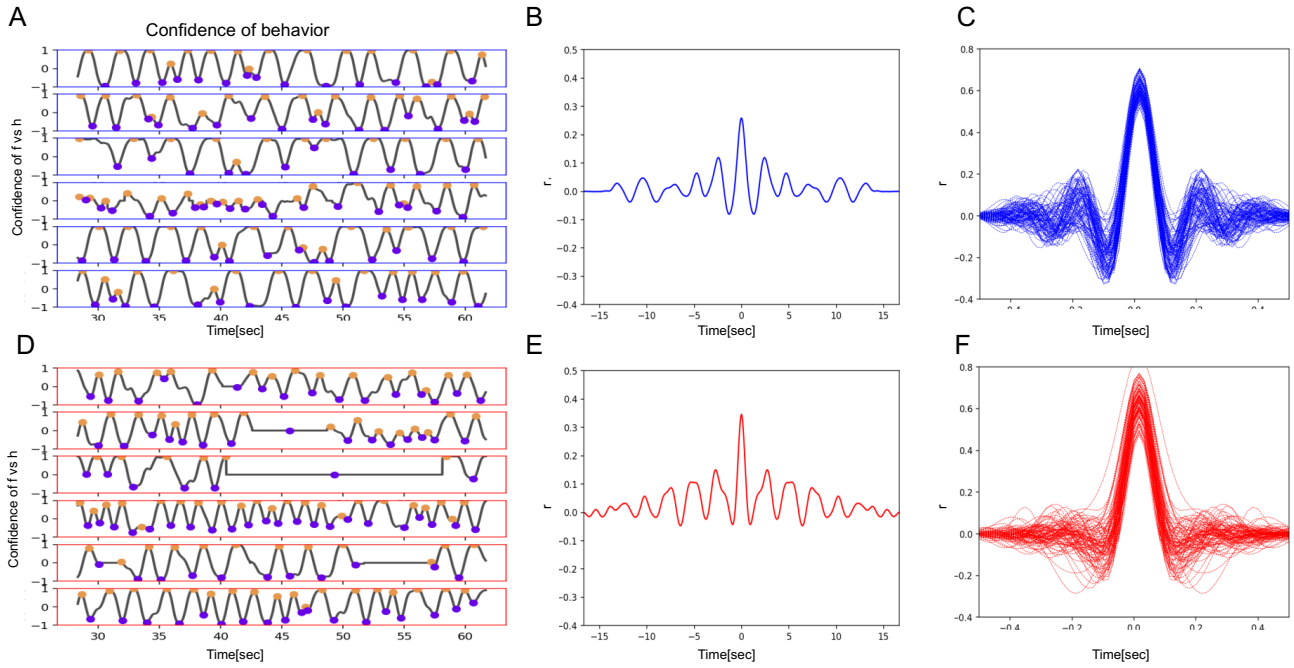

Supplementary Figure 2: Bout alternations remain periodic across a range of temperatures

(**A**) Samples of five flies recorded at low temperature (18ºC, blue frame), showing behavior confidence curves with several ff/hh cycles. Purple and orange circles indicate the times of h- and f-peaks. (**B**) Autocorrelation function curves of behavior confidence sampled from 18ºC flies, indicating strong periodicity of the signals (side peaks). (**C**) Samples of autocorrelation functions (ACF) computed from over 8 minutes of a movie when the fly was engaged in front leg rubbing or head sweeps. (**D**)-(**F**) Same as A-C but for high temperature (30ºC).

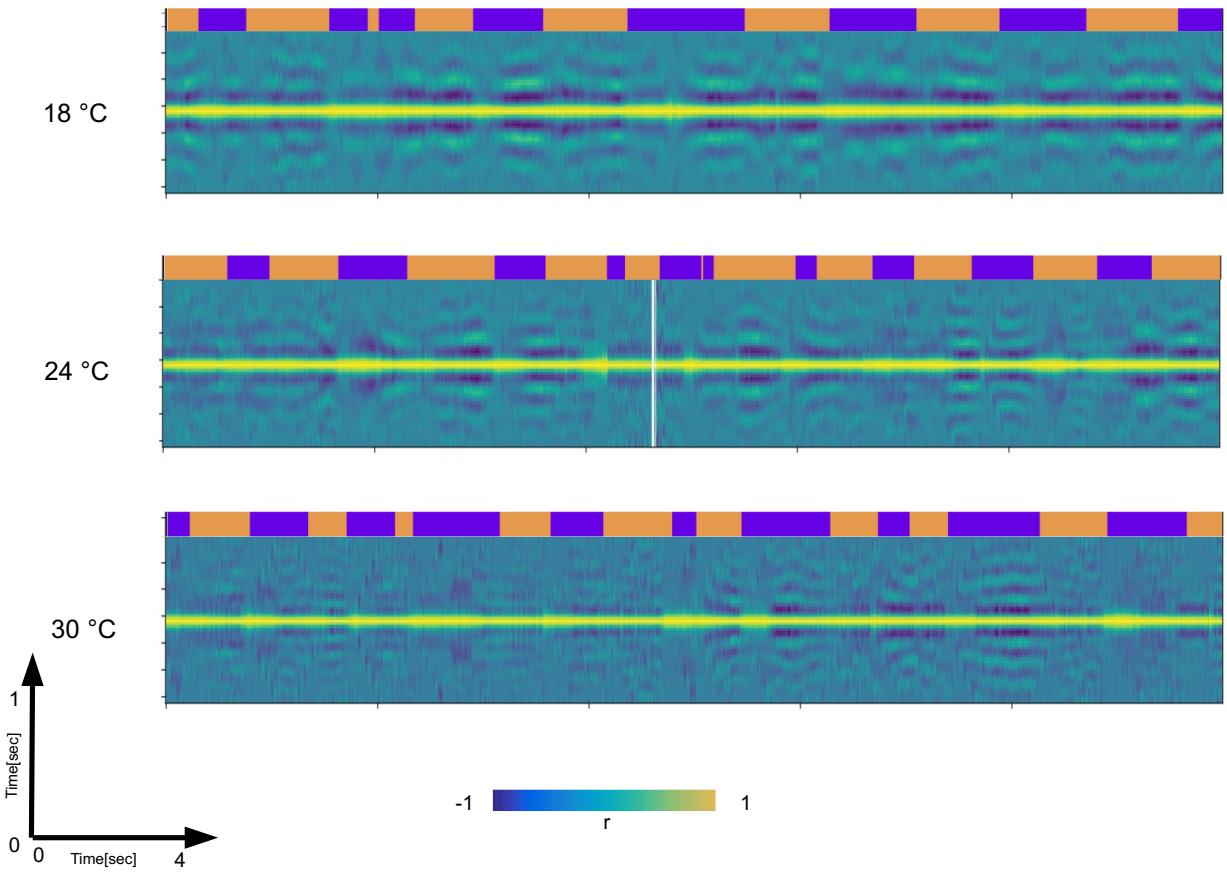

Supplementary Figure 3: Autocorrelation analysis show temperature driven contraction across time-scales

Autocorrelation functions (ACFs) computed from 0.5 sec windows of raw videos of dusted flies are stacked together as columns into matrices across ~17 seconds of a movie. Each matrix is showing the change of ACF shape across the ~17 seconds. Note the modulation of the side-band positions and their numbers which is reflective of frequency modulation on the short time-scale (y-axis). Also note the modulation of the longer time-scales (x-axis). The three matrices shown are taken from different temperatures. Note that at the highest temperature the y-axis becomes "denser" (more side-bands) and that the episodes of harmonic bouts become shorter (x-axis). This way we can observe simultaneous transformation of x-axis and the y-axis as a result of temperature increase. The ethograms on top of the matrices are used as a reference.

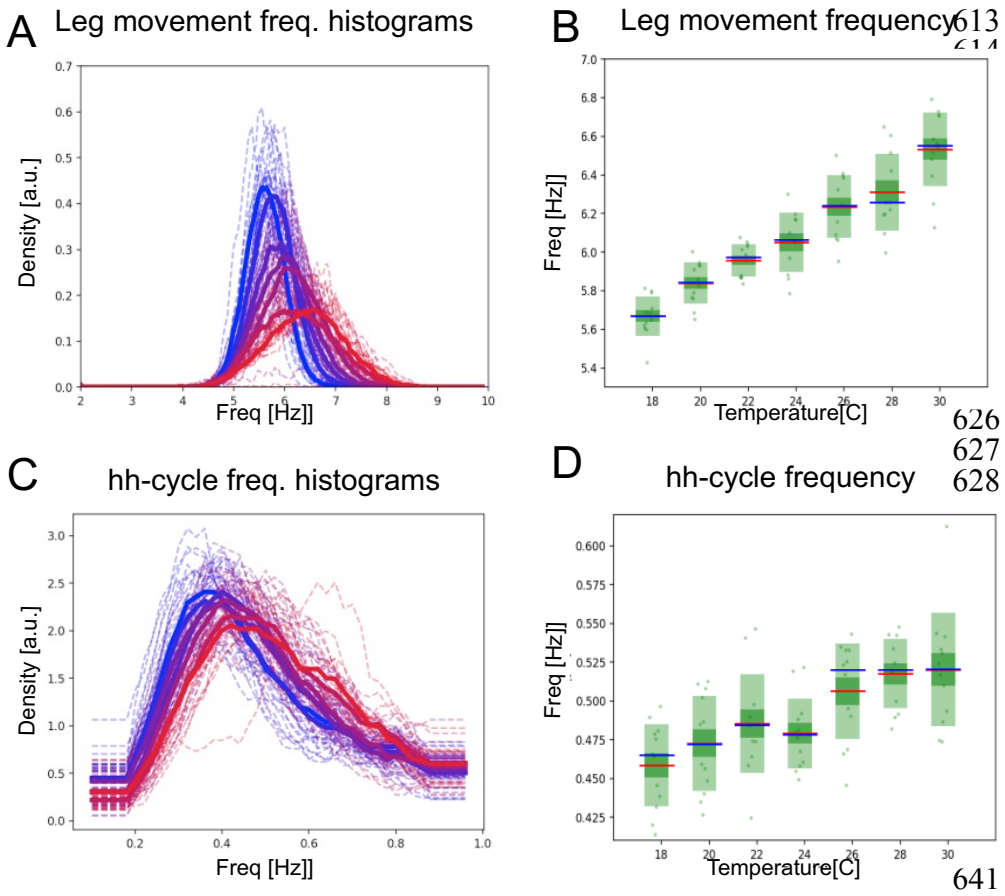

Supplementary Figure 4: The hh-cycles also contract with increasing temperature

(**A**) Histograms of mean frequencies at cool (blue) and warm (red) temperatures, and (**B**) box plots of the increase in leg movement frequency with temperature; plots and statistics as described in **Figure 2C, D,** and **E.** **(C)** Long-time scale hh-cycle analysis comparable to **Figure 2** and **3 G** and **H**.

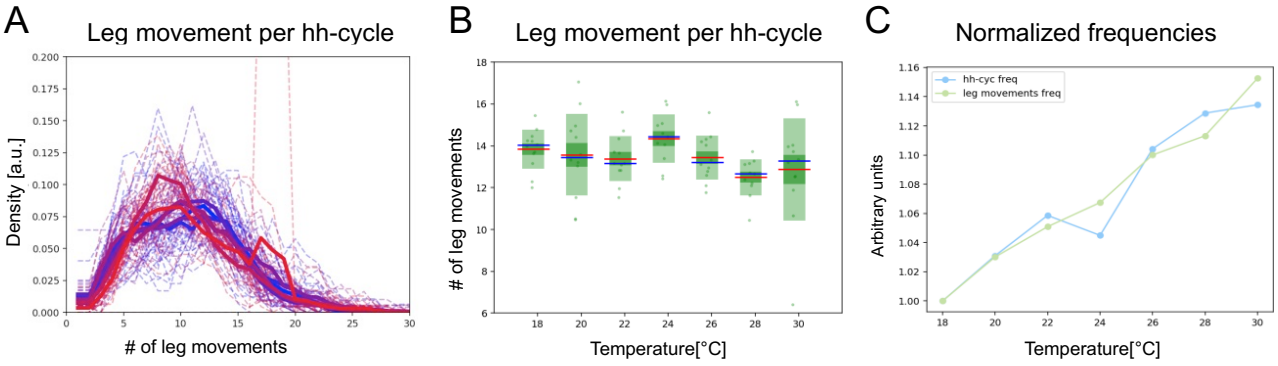

Supplementary Figure 5: Head sweeps and hh-cycles contract at the same rate as temperature increases

(**A**) Histograms of numbers of leg movements per hh-cycle in cooler temperatures (blue) and warmer temperatures (red). (**B**) Box plots of leg movement counts per hh-cycle across the seven temperatures; statistics as in **Figure 2E**. (**C**) The frequency of individual leg movements and bout alternations (hh-cycles) increases roughly linearly with temperature but over different time-scales (msec vs. sec; 7Hz vs. 0.5Hz).

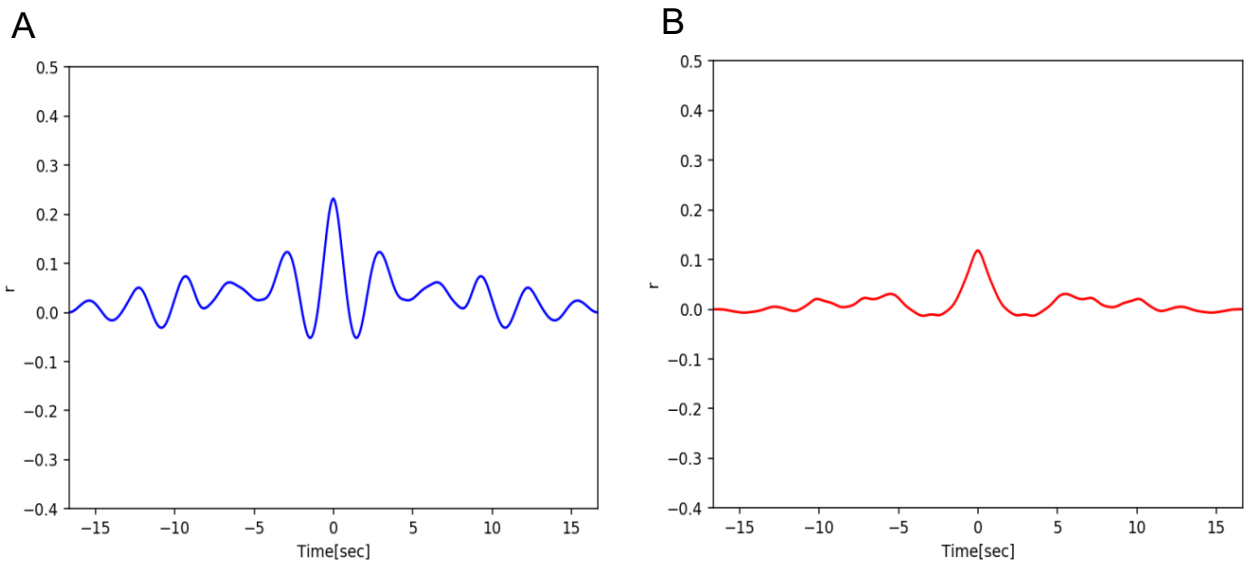

Supplementary Figure 6: Bout alternations remain periodic across a range of temperatures in optogenetically-stimulated flies

(**A**) Autocorrelation function curves of behavior confidence sampled from 18ºC flies, indicating strong periodicity of the signals (side peaks). (**B**) Same as **A** but for high temperature (30℃). The autocorrelations here are lower than in **A**, however side-peaks remain.